Photon-Counting Technologies for Efficient High-Capacity Space-to-Ground Laser Communications§

D. O. Caplan*, Z. J. Darling, M. E. Grein, M. Guyton, D. Russo, B. Tyrrell, A. Wagner
MIT Lincoln Laboratory, 244 Wood Street, Lexington, MA 02420, USA
*Author e-mail address: *doc@ll.mit.edu*

Abstract: Photon-counting optical receivers have the best sensitivity but are practically limited to relatively low data rates < ~1 Gbit/s. Here, we present technologies that can extend sensitive photon-counting-performance into the 100 Gbit/s regime and beyond. @ 2024 The Author(s)

1. Introduction

Photon-counting receivers (RXs) have the best known sensitivity in theory [1, 2] – making them attractive for power-starved applications such as free-space optical (FSO) communications [3-8], especially for links through the atmospheric channel where multimode detection enables more-efficient collection of aberrated multi-spatial-mode wavefronts [9] without the need for complex and expensive adaptive optics (AO) used in conventional single-mode RXs (e.g., [10]). However, photon counting RXs are often constrained by inadequate detector bandwidth, limiting them applications with low photon flux to avoid significant detector saturation and blocking-loss penalties [11]. In practice, this has limited photon counting RXs to low data rate < ~1 Gbps [3-9] and low background noise applications that require larger Sun-Earth-Probe angles [12].

In this paper, we present three technologies under development that enable photon counting RXs that can scale to support sensitive high-capacity 100 Gbps class laser communications. These include: 1) agile power-efficient laser transmitters (TXs) that can generate high-fidelity optical waveforms over many wavelength division multiplexed (WDM) optical channels with good size, weight, and power (SWaP) efficiency; 2) low-loss narrowband multimode WDM matched optical filters that remove out-of-band background and efficiently distribute incoming WDM signal waveforms across the elements in the photon-counting detector array; and 3) high-speed large-pixel-count superconducting nanowire single photon detector (SNSPD) arrays enabled by a superconducting-logic-based read out integrated circuit (ROIC). The combination of these with hybrid orthogonal photon counting (HOPC) communication formats can yield versatile lasercom capabilities with an unprecedented combination of speed and sensitivity.

2. Agile Laser Transmitters

A block diagram of the TX and RX configuration is shown in Fig. 1A [13]. On the TX side, time- and frequency-windowed directly modulated lasers (DMLs) can efficiently generate a variety of wavelength division multiplexed (WDM) optical waveforms with good fidelity and low drive power (< 100 mW) per WDM channel (λ) [14]. This enables power-efficient WDM scaling to a large number of λs, while maintaining low-SWaP implementation.

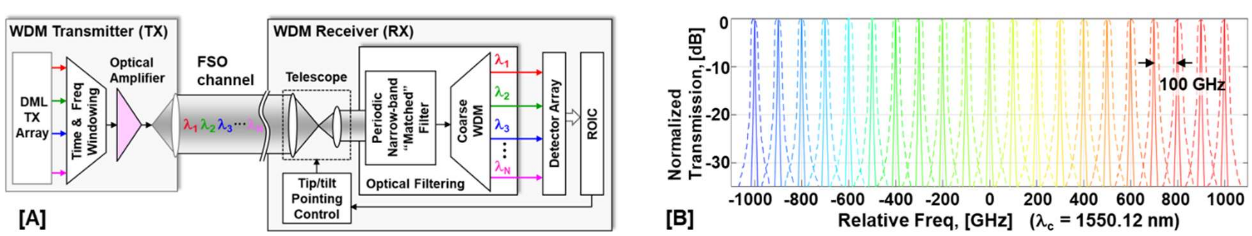

Fig. 1. [A] WDM TX and RX block diagram. **[B]** Measured optical filter transmission, showing filtered output from 21 of 32-WDM channels with 100 GHz spacing and 30 GHz bandwidth (dashed), and cascaded filtering with narrow 3 GHz passbands (solid).

3. WDM Matched Optical Filters

On the RX side, low-loss WDM optical filtering technologies can enable existing photon-counting detector technologies to support high-speed and high-sensitivity photon-counting reception – while eliminating existing noise, bandwidth, and other limitations [13]. Multi-spatial-mode photon-counting detection simplifies reception of weak optical signals through the turbulent atmospheric channel (e.g.,[9]), but this increases background noise, which grows with the number of spatial modes – degrading the RX signal-to-noise ratio and increasing blocking-loss penalties [5, 11, 15]. To balance FSO coupling and background noise concerns, the number of spatial modes is limited to < 30, while the impact of unwanted background is reduced via narrow-band optical filtering – which ideally attenuates out-of-band noise modes and passes multimode RX signal with minimal loss. As shown in the WDM RX of Fig. 1A, a cascaded filter design is used to implement low-loss narrowband WDM optical filtering to minimize the impact of background noise while providing efficient channelized access to many THz of available optical spectrum in the telecom C-band at 1.55μm [13]. Multimode WDM optical filtering is realized with 3 GHz and 30 GHz passbands for cascaded and coarse optical filtering – which are well matched to Gaussian-like return-to-zero waveforms with ~1 ns and 10 ns signal pulse durations, respectively [4].

Note that while WDM techniques provide a straightforward way to increase photon-counting RX data rate, high-speed large-pixel-count SNSPD arrays enabled by cryogenic ROICs are essential for efficient scaling to the 100 Gbps regime.

4. High-speed large-pixel-count SNSPD arrays with a superconducting ROIC

SNSPDs have nearly ideal photon-counting characteristics in the near infrared with extremely low dark counts (< 100 Hz) and timing jitter (< 100 ps), short reset times (< ~5ns), and good detection efficiency (> ~75%) [3, 6, 8, 9, 16]. In contrast with Geiger-mode APDs that have been used for low data rate applications < ~50 Mbps [5], SNSPD-based RXs have demonstrated nearly 1 Gbps data rates with ~1 photon/bit sensitivities (e.g., [3, 6]). However, scaling SNSPD-based RXs to support higher data remains a challenge since processing their signals requires readout and amplification to room temperature ADCs and processors. State-of-the-art SNSPD-based lasercom RXs use one RF cable to relay photon-arrival times to external read-out and processing electronics for each detector (e.g., [6-8]). In addition to creating a substantial thermal load – which practically constrains the detector array size to ≤ 64, this adds tremendous size and complexity to SNSPD array systems, limiting their utility despite the promise of the underlying detector technology. An attractive solution to this problem is to process the received SNSPD signals with a ROIC within the cryogenic environment. This is difficult to achieve with CMOS technology however superconducting logic families based on Josephson junctions (JJ) provide an attractive route.

Josephson logic families exploit the nonlinear switching behavior of superconducting JJ weak links to modulate the distribution of current in superconducting loops constituting the logic circuit. The states of the circuit correspond to one of two quantized distributions of current within a particular logical element. Switching speed is extremely high, ~480 GHz, and the switching energy extremely low, ($< 10^{-19}$ J/bit) [17], orders of magnitude more efficient than CMOS. Logic gates and even larger processors have been demonstrated in this technology with clock speeds up to 153 GHz [18]. This speed and efficiency of JJ-based logic circuits, when coupled with their extremely high sensitivity to magnetic flux and low noise make them ideal for direct digitization of SNSPD pulses. This concept has recently been implemented to demonstrate a cryogenic digital signal processor for an SNSPD imaging array [19, 20].

Josephson-based ROICs can address practical challenges of implementing SNSPD-based high-data-rate photon-counting RXs in two significant ways. First, they can enable efficient aggregation of photon detections from many SNSPDs, which can dramatically reduce the input/output connections (I/O) and corresponding thermal load. Second, they enable the use of multi-level signaling to further reduce both I/O bandwidth and number of cable connections. For example, a ROIC receiving a high-photon-flux 100 Gbps signal with 1 photon/bit would need to support a 100 GHz count rate. To limit blocking loss to < 0.5 dB for SNSPDs with reset time $\tau_r = 3$ ns, this would require SNSPD-arrays with $N \gtrsim 10 \cdot \tau_r \cdot \text{count rate} = 3000$ detectors. This would be prohibitively complex using the one-cable-per detector paradigm, but by aggregating ≥ 64 detectors per I/O – the external interface can be greatly simplified, with the total number of data I/O for this high-flux scenario reduced to < 50 connections and manageable thermal load. In addition, 10 ps photon arrival time resolution could be relayed on a single 25 GHz I/O by using 16-level (4-bit) output signaling, further simplifying the external interface.

5. Hybrid orthogonal photon counting (HOPC) Performance

Combining these TX and RX capabilities with time- and frequency-based hybrid-orthogonal modulation enables robust high-sensitivity performance in the presence of background over a wide range of rates that can scale to 100 Gbits/s and beyond. Fig. 2 shows the wide operational rate-sensitivity trade space for a 10 GHz bandwidth-limited max slot rate photon-counting RX under development with rate-½ coding – as the orthogonal symbol size, M, varies from 2 (binary, with one bit/symbol) to 1024 (with $\log_2 M = 10$ bits/symbol). As M grows, sensitivity improves by up to 10 dB. For a power-starved link, this sensitivity gain could enable up to a 10x increase in data rate or, alternatively, a 10x reduction in effective TX-RX power-aperture product that could be leveraged to lower system SWaP and cost.

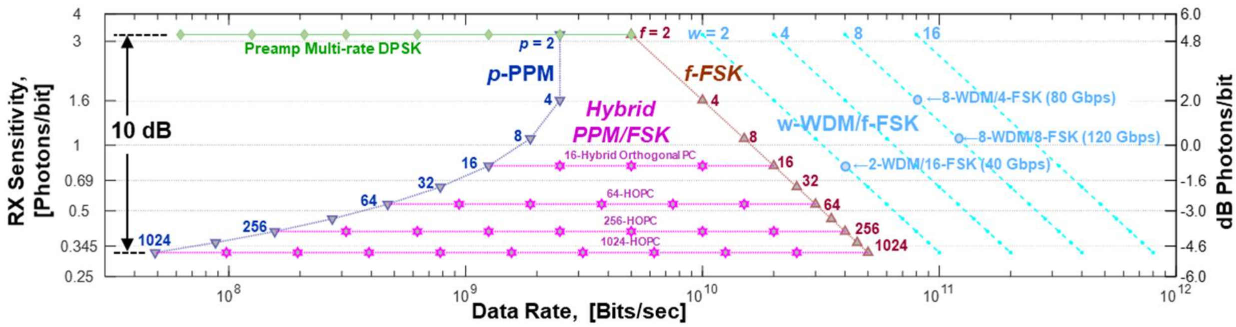

Fig. 2. Ideal photon counting sensitivity versus data rate for 10 GHz modulation and rate-½ coding. Blue downward triangles (M-PPM), Red triangles (M-FSK), Magenta stars (hybrid M-orthogonal PPM/FSK), Light-blue dashed lines, (WDM/FSK). Green diamonds (Multi-rate DPSK). Note that the 10 GHz max slot rate (corresponding to 100 ps timing resolution) was selected for convenience in this analysis; anticipated detector-array timing jitter and ROIC-limited resolution may support up to 100 GHz rates that could proportionally scale resulting data rates by 10x.

Commonly used M-ary pulse position modulation (M-PPM) is better suited for lower-rate applications since the data rate $\propto \log_2 M/M$ decreases as M grows. However, peak power also grows with M, which often limits M to ≤ 128 to avoid peak-power-induced TX nonlinear impairments or modulation extinction ratio (ER) penalties. On the other hand, the rate for M-ary frequency shift keying (M-FSK) grows with M with constant peak power, making M-FSK better-suited for higher-rate or peak-power-limited applications. By adjusting the number of frequencies (f) and positions (p), the effective constellation size $M_{\text{eff}} = p{\cdot}f$ can be adjusted to accommodate a variety of data rates, sensitivities, and practical limitations [4, 13]. Furthermore, conventional WDM can also be employed so rates scale linearly with the number of independent WDM channels, w. For example, a 32-FSK RX could support up to 25 Gbps with -1.9 dB photon/bit sensitivity. Alternatively, 32-λs could be used for 4-WDM/8-FSK at 60 Gbps and 0.31 dB photon/bit sensitivity; extending to 64 λs using 8-WDM/8-FSK enables 120 Gbps with the same sensitivity. For higher sensitivity to support communication over more challenging links, 1024-HOPC using 32-PPM/32-FSK can be employed at 1.6 Gbps with -4.9 dB photon/bit (~3 bits/photon) sensitivity that requires only modest ER and peak power handling.

In summary, we have presented agile laser TX and RX technologies that can efficiently channelize and leverage available optical spectrum to achieve high-sensitivity performance over a wide range of data rates. Furthermore, we have introduced an approach for realizing large-pixel-count high-speed SNSPD-arrays enabled by Josephson-based ROICs that provide a path to ultra-sensitive 100+ Gbps photon-counting RXs. Such capabilities enable scalable and extensible high-performance solutions for lasercom through the dynamic FSO channel suitable for a variety of future SWaP and performance-constrained space-to-ground applications.

6. References

[1] J. P. Gordon, "Quantum Effects in Communications Systems," *Proceedings of the IRE,* vol. 50, pp. 1898-1908, 1962.
[2] J. R. Pierce, et al., "The Capacity of the Photon Counting Channel," *IEEE Trans. Info. Theory,* vol. IT-27, pp. 61-77, Jan. 1981.
[3] B. S. Robinson, et al., "781-Mbit/s Photon-Counting Optical Communications Using Superconducting NbN- ..." *Opt. Lett.,* 2006.
[4] D. O. Caplan, "Laser communication transmitter and receiver design," *J. Opt. Fiber Commun. Res.,* vol. 4, pp. 225–362, 2007.
[5] J. A. Mendenhall, et al., "Design of an Optical Photon Counting Array Receiver System for Deep Space Comm," *Proc. IEEE,* 2007.
[6] D. M. Boroson and B. S. Robinson "The Lunar Laser Communication Demo NASA's First Step ..." *Space Sci. Rev. Journal,* 2014.
[7] F. Khatri, et al., "Space-to-Ground Optical Interface Verification for Orion Artemis II Optical (O2O) Comm ..." *IEEE ICSOS,* 2023.
[8] R. Rogalin, et al., "A high dynamic-range photon-counting receiver for deep space optical communication," *SPIE,* vol. 11678, 2021.
[9] M. E. Grein, et al., "A multimode fiber-coupled photon-counting optical receiver for the LLCD," in *CLEO*, 2014, p. SM4J.5.
[10] P. Thompson, et al., "NASA's LCOT (low-cost optical terminal) ..." *SPIE LASE,* vol. 12413, 2023.
[11] D. Rosenberg, et al., "High-speed and high-efficiency superconducting nanowire single photon detector array," *Opt. Expr.,* 2013.
[12] A. Biswas, et al., *LLCD operations using the Optical Communications Telescope Laboratory (OCTL)* vol. 8971: SPIE, 2014.
[13] D. O. Caplan and Z. J. Darling, "Enabling Technologies for Space-based Lasercom," in *Optica Adv. Photonics Congress (APC)*, 2022.
[14] D. O. Caplan, et al., "WDM Laser Transmitters for Mobile Free-space Laser Communications," *Proc. SPIE,* vol. 9739, 2016.
[15] D. Boroson, "Performance limits and simplified analysis of photon-counted noisy free-space optical links," *Proc. SPIE,* 2018.
[16] F. Najafi, et al., "Fabrication Process Yielding Saturated Nanowire Single-Photon Detectors With 24-ps Jitter," *IEEE JSTQE,* 2015.
[17] D. S. Holmes, et al., "Energy-Efficient Supercond Computing - Power Budgets and Reqs," *IEEE Trans on Appl Supercond.,* 2013.
[18] M. Tanaka, et al., "Rapid Single-Flux-Quantum Circuits Fabricated Using ..." *IEEE Transactions on Applied Superconductivity,* 2015.
[19] S. Miyajima, et al., "High-time-resolved 64-channel single-flux quantum-based address encoder integrated ..." *Opt Expr,* 2018.
[20] M. Yabuno, et al., "Scalable implementation of a SNSPD array with a superconducting digital signal processor," *Opt Expr,* 2020.